Discussion on VIS Inertial Sensor Sensitivity Requirement for Post-O3 Upgrade

Tsang Terrence Tak Lun
The Chinese University of Hong Kong

April 9, 2020

Abstract   The current configuration of the feedback system at the inverted pendulum stage utilizes only LVDTs with sensor correction. A conservative residual motion requirement of the inverted pendulum was derived from such configuration under the condition of 50th percentile seismic noise. Under this requirement, the inverted pendulum residual displacement should be less than $0.0128\,\mu\text{m}$ in terms of band limited integrated RMS within $0.1\,\text{Hz}$ to $1\,\text{Hz}$. The total integrated RMS figure is not as representative due to noise amplification of sensor correction and complementary filter at lower frequencies, but it was included for reference anyway.

Complementary filters and control gain were optimized for a list of different geophone noise level under different conditions. Noise level was taken from the list as the requrement under the condtion if the optimal filters give a simulated residual motion meeting the aforementioned requirement.

Without sensor correction, it requires the inertial sensor noise to be impractically low in order to meet the requirement. With sensor correction of 40% inter-calibration mismatch, the geophone noise requirement is the noise 21% lower than the typical geophone noise under 50th percentile seismic noise. It would as well require the sensor noise to be unrealistically low under 90th percentile seismic noise under this condition. With 10% of mismatch, the typical geophone noise level should be sufficiently low under ground motion of 50th percentile, whereas the required geophone noise level is 15% lower than that of the typical geophone noise under 90th percentile seismic motion.

With the typical geophone noise level, the tolerable sensor correction inter-calibration mismatch is 7%. If inter-calibration error of less than 7% is achievable, then upgrading inertial sensors is not necessary. This means that it is possible to withstand 90th percentile ground disturbance with current hardware if the implementation if sensor correction is good enough. Therefore, it is very crucial to implement sensor correction in the near future.

Under 50th percentile seismic noise, the optimal gain is around 3 times higher than the current gain of the ITMY inverted pendulum and is around 30 times higher under 90th percentile ground noise. In the latter case, the filter must be reshaped since the optimal gain exceeds the gain margin. Nevertheless, the drastic changes in optimal gain strongly encourages adaptive control. This should also be considered.

1 Introduction

Inability to withstand high seismic motion has been a long standing issue for KAGRA. High seismic activity causes the increase of mirrors residual displacements, causing difficulty for stable cavity lock. In principle, seismic noise at low frequencies should be actively damped by the feedback controls at the preisolator stage. Efforts have been made to implement complementary filters to integrate inertial sensors for such controls. However, we were not able to gain satisfactory performance from the implementation due to the low noise performance of inertial sensors at low frequencies. In particular, the blending frequency cannot be tuned to be substantially lower than the secondary microseism frequency ($<$ 150 mHz), without causing issues to the control system. Later, we switched focus to utilize sensor correction to the relative displacement sensors (LVDTs), which seemed to be effective in suppressing seismic motion by some 0 to 1 orders of magnitude [7]. However, lock-loss due to high ground motion were still experienced during commissioning. So, better seismic suppression is seemingly needed at the preisolator stage and some proposed upgrading the inertial sensors. Here, we discuss the sensitivity requirement of inertial sensors as we consider to upgrade our inertial sensors.

We emphasize that the current seismic noise performance is not the best of what our current system is able to achieve and we blame the lack of time. To list, we should be able do better by: optimizing the sensor correction gain, implementing sensor corrections for all ground coupled sensors including but not limited to LVDTs at the bottom filter and optical levers, implementing seismometer feedforward and optimizing the damping filters or implementing adaptive optimal filters as described in JGW-G1911004. In particular, we can obtain an over-simplified control gain by Eqn. 6 in the document. Using ITMY as an example, when the seismic noise is as high as $1 \, \mu\text{m}/\sqrt{\text{Hz}}$ at 0.21 Hz and assuming that the sensor noise is $10^{-1} \, \mu\text{m}/\sqrt{\text{Hz}}$, and that the actuation efficiency is 0.2, the optimal loop gain is 2000, where as the current loop gain only go as high as a conservative 20 at the particular frequency.

We also emphasize that having better inertial sensors alone will not help suppressing high seismic noise. It has to be combined with good complementary filter and good control filter in order to be useful. For the following analysis, we propose a method to obtain good filters, which will be useful in defining the sensor noise requirement.

2 Noise Models

For the following analysis, we will assume some noise models for simplicity unless otherwise specified.

2.1 Sensor Noise

The noise profile in terms of ASD for the relative sensors and inertial sensors is defined as

$$
N_s = \begin{cases} N_0 f^a & , f < f_c \\ \left[N_0 f_c^{(a-b)} \right] f^b & , f > f_c \end{cases} \frac{\mu\text{m}}{\sqrt{\text{Hz}}}.
\tag{1}
$$

Here, a and b are the exponents of the noise profile before and after some corner frequency f_c, respectively. The factor $f_c^{(a-b)}$ is required in the second expression for continuity. And, N_0 is some constant defining the overall noise level of the noise ASD. Table. 1 are some typical values for LVDTs and geophones.

	N_0	a	b	f_c
LVDT	$8 * 10^{-3}$	-0.5	0	4.5
Geophone	$2 * 10^{-6}$	-3.5	-1	0.9

Table 1: Typical values describing the ASD of LVDT and geophone noise. Values are directly derived from plots in Sekiguchi's thesis [6].

2.2 Seismic Noise

A model of seismic noise including low frequency microseism is not readily available as of March 19, 2020. But, we can directly use the one-year data measured by Miyo [4].

2.3 Seismometer Noise

The self-noise of Trillium Compact seismomter, the seismometer used at the central area in KAGRA, is specified by the manufacturer's user-guide, available at [1] or at their website [5]. I picked some data points from the data sheet and did a piece-wise linear interpolation in log-scale to give the overall noise profile of the seismometer.

2.4 Noise summary

As a sanity check, the values for LVDT and geophone noise agree with the measurements done by Lucia, see klog 8568 [9] and 7344 [10], with one exception: The LVDT noise for ETMX is around $10^{-3}\,\mu\text{m}/\sqrt{\text{Hz}}$ above 1 Hz, intead of the typical $10^{-2}\,\mu\text{m}/\sqrt{\text{Hz}}$. This means that we are potentially dealing with pessimistic estimations when using the typical level.
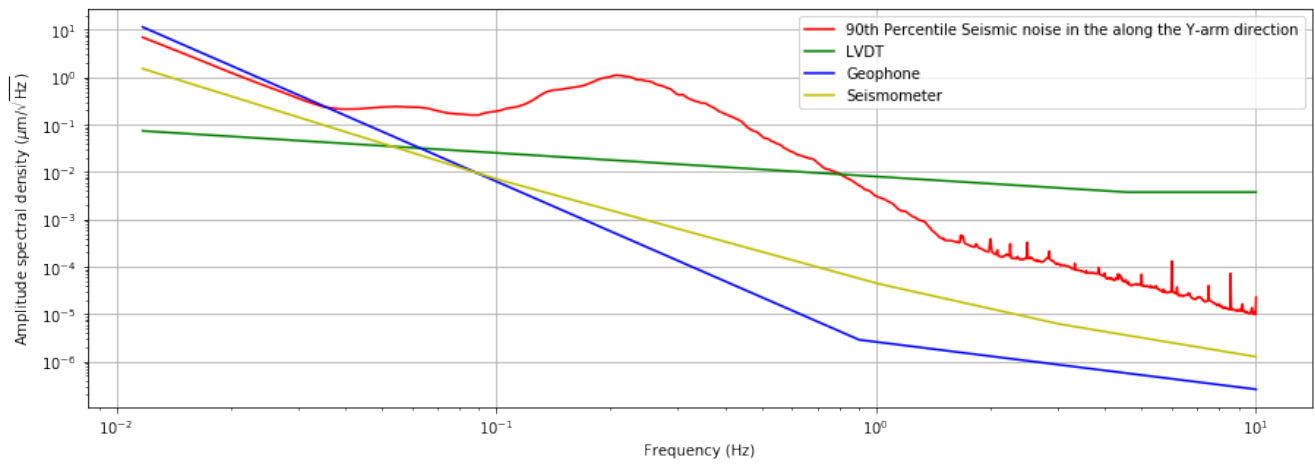
Figure 1: A summary of typical sensor noises and the 90th percentile seismic noise at KAGRA.

3 Strategy

From experience, we know for a fact that lock-loss due to seismic noise happens when the seismic noise level is high. This means that we can safely assume that, under the current control configuration, our system is able to sustain at least some level of seismic noise to an extent where lock-acquisition is possible. Therefore, we can set a residual motion requirement as the residual motion under this condition. Then, we would be able to discuss the sensor noise requirement under some slightly adverse conditions.

3.1 Residual Displacement Requirement of the Preisolator
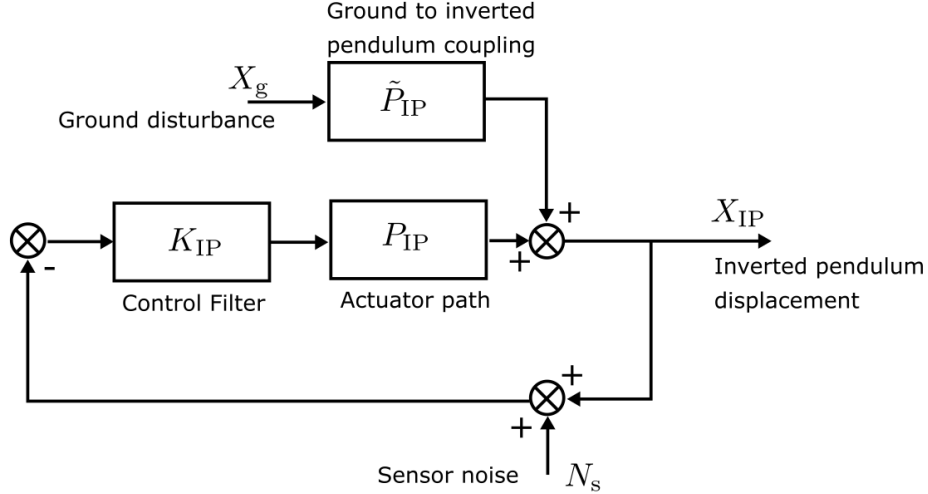
Figure 2: The control block diagram describing the signal flow of the inverted pendulum feedback system

Under feedback control as described in Fig. 2, the displacement of the inverted pendulum X_{IP} can be written as

$$X_{\mathrm{IP}} = \frac{1}{1 + K_{\mathrm{IP}} P_{\mathrm{IP}}} \left(\tilde{P}_{\mathrm{IP}} X_{\mathrm{g}} \right) - \frac{K_{\mathrm{IP}} P_{\mathrm{IP}}}{1 + K_{\mathrm{IP}} P_{\mathrm{IP}}} N_{\mathrm{s}}, \tag{2}$$

where K_{IP} is the control filter, P_{IP} is the actuation path of the inverted pendulum, $\tilde{P}_{\mathrm{IP}}$ is the ground to inverted pendulum path and can be approximated by P_{IP} normalized at DC, i.e. $\tilde{P}_{\mathrm{IP}} \equiv \frac{1}{|P_{\mathrm{IP}}(0)|} P_{\mathrm{IP}}$, X_{g} is the ground motion and N_{s} is some generic sensor noise. Fig. 2 shows the control configuration of the preisolator.

Here, the amplitude spectral density of the inverted pendulum displacement is the quadrature sum of the filtered ground motion and the filtered noise, given by

$$\sqrt{\langle X_{\mathrm{IP}}^2 \rangle} = \sqrt{ \left| \frac{\tilde{P}_{\mathrm{IP}}}{1 + K_{\mathrm{IP}} P_{\mathrm{IP}}} \right|^2 \langle X_{\mathrm{g}}^2 \rangle + \left| \frac{K_{\mathrm{IP}} P_{\mathrm{IP}}}{1 + K_{\mathrm{IP}} P_{\mathrm{IP}}} \right|^2 \langle N_{\mathrm{s}}^2 \rangle }. \tag{3}$$

In the current situation described in Fig. 3, the inverted pendulum utilizes a sensor correction path to reduce seismic noise coupling to the LVDT signals. Hence, the total sensor noise is $N_{\mathrm{s}} = N_{\mathrm{LVDT}} + H_{\mathrm{sc}} N_{\mathrm{seis}} + (H_{\mathrm{sc}} - 1) X_{\mathrm{g}}$, where N_{LVDT} is the intrinsic noise of the LVDT, H_{sc} is the sensor correction path and N_{seis} is the seismometer noise. It follows that the ASD of the sensor noise is $\sqrt{\langle N_{\mathrm{s}}^2 \rangle} = \sqrt{\langle N_{\mathrm{LVDT}}^2 \rangle + |H_{\mathrm{sc}}|^2 \langle N_{\mathrm{seis}}^2 \rangle + |(H_{\mathrm{sc}} - 1)|^2 \langle X_{\mathrm{g}}^2 \rangle}$. Plugging the transfer functions for the current ITMY, we get the residual motion as shown in Fig. 4

From Fig. 4, the simulated performance of the current control system of the ITMY inverted pendulum shows that the integrated RMS/expected RMS, defined by

$$\mathbb{E}\left(\sqrt{\langle X_{\mathrm{IP}}^2 \rangle} \right) \equiv \sqrt{ \int_0^\infty \langle X_{\mathrm{IP}}^2 \rangle \, df }, \tag{4}$$
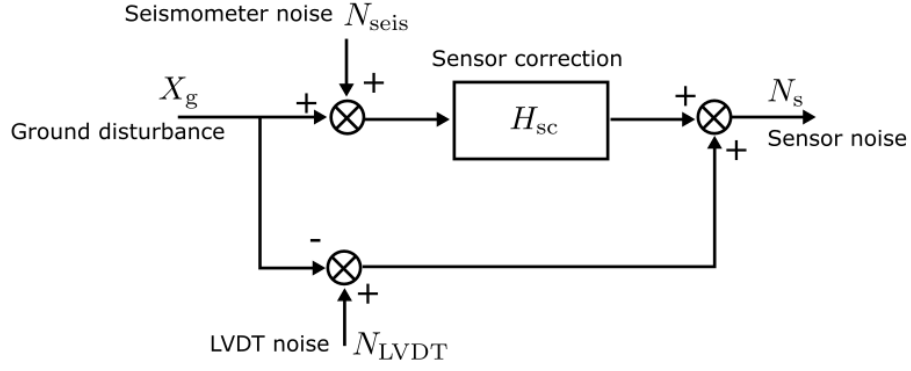
Figure 3: Sensor noise of the current sensor correction configuration.
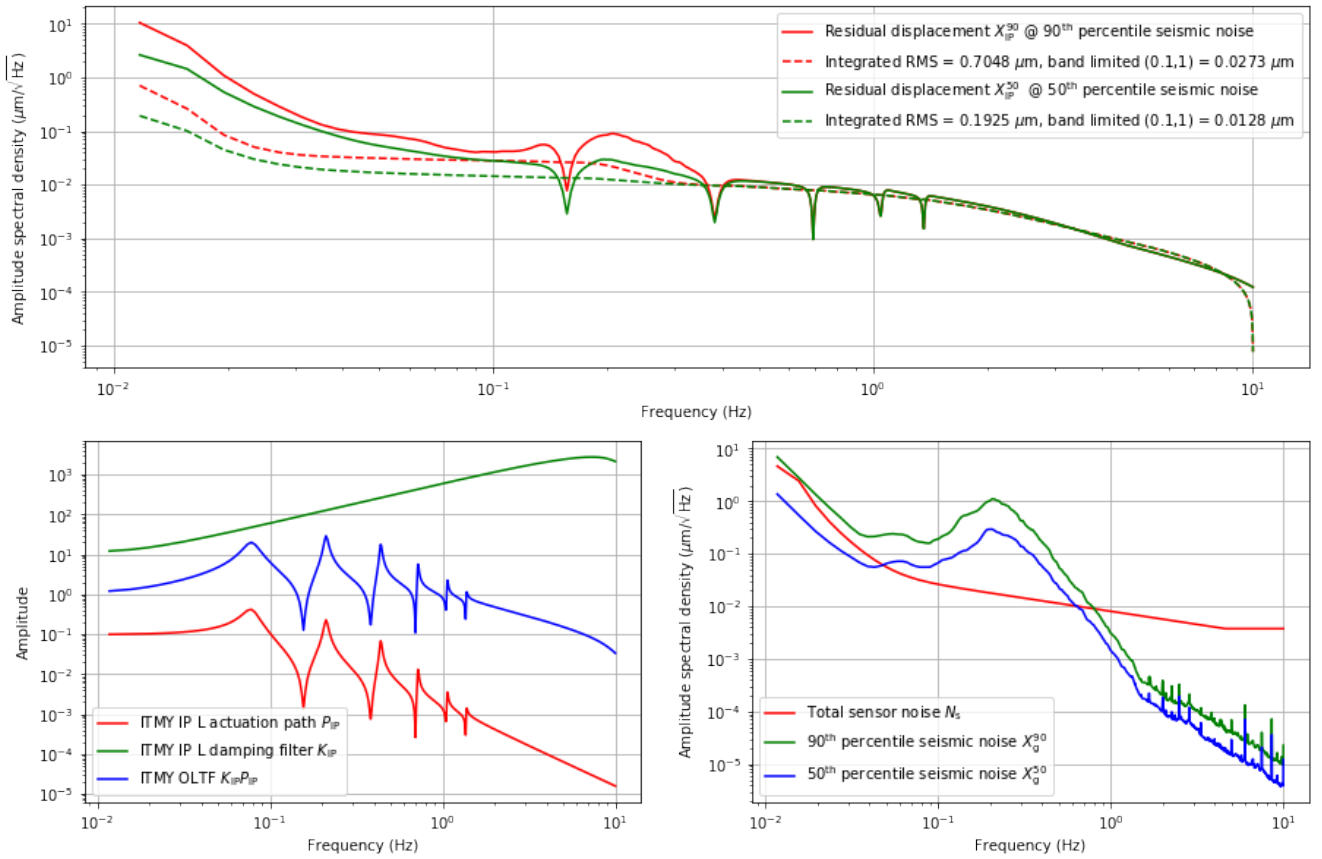
Figure 4: Top: The residual motion of the inverted pendulum under 50th and 90th percentile seismic noise and under current damping filter. Bottom left: The longitudinal damping gain and actuation path of the ITMY inverted pendulum. Bottom Right: The reference sensor noise and seismic noises.

under 90th and 50th percentile seismic noise is $0.7048\,\mu\text{m}$ and $0.1925\,\mu\text{m}$ respectively. From the top figure, the expected RMS increased drastically at frequency range from $0.1\,\text{Hz}$ to $0.01\,\text{Hz}$, whereas the expected RMS remains approximately flat at frequencies bounded by the microseism frequency. At lower frequencies, the inverted pendulum control has high gain for coarse alignment anyway. So, if we integrate the spectra to even lower frequencies, the integrated RMS will increase almost indefinitely which might not be useful for analysis. Therefore, we can set another reference by the band limited integrated RMS which encloses the spectra from $0.1\,\text{Hz}$ to $1\,\text{Hz}$. We choose the lower limit this way because noise lower than $0.1\,\text{Hz}$ are very hard to get rid of but are usually acceptable. Our sensor correction filter as well as LIGO's has noise amplification at range lower than $0.1\,\text{Hz}$ [3]. If we expect the

complementary filter to blend at frequencies between $0.01\,\mathrm{Hz}$ and $0.1\,\mathrm{Hz}$, then almost certainly we will expect to see noise amplification around the frequency range as well. To mitigate such undesirable amplification we must use notches in the control filter if necessary. Nevertheless, we choose the upper limit to be $1\,\mathrm{Hz}$ so this ensures that the secondary microseism, which is usually most problematicm, is taken into account.

From the figure, the band limited RMS under 90th and 50th percentile ground motion is $0.0273\,\mu\mathrm{m}$ and $0.0128\,\mu\mathrm{m}$ respectively. These values are much closer to the known residual motion requirement stated in Sekiguchi's thesis. Assuming that the motion of the inverted pendulum at lower frequencies transfers to the test mass without passive attenuation, we can compare directly the residual motion at the IP to that of the TM. Sekiguchi estimated the residual motion requirement for the test masses to be $0.01\,\mu\mathrm{m}$ [6]. This estimation is known to be very conservative as it solely depends on the actuation capability of the test mass stage. In practice, the more powerful actuation from upper stages was also utilized for lock-acquisition. Therefore, the requirement can be slightly eased. However, it will be very tedious and difficult to estimate the actual requirement. From experience, we know that lock-acquisition is possible at nominal condition. Therefore, we directly use the simulated residual motion of the IP under 50th percentile seismic noise as a reference for the residual motion requirement for the IP.

3.2 Complementary Filter Optimization

The inertial sensor is intrinsically AC-coupled. Therefore, it only works at higher frequencies and requires a high-pass filter to work with. This filtered signal is not completed because it is missing the low frequency content of the measurement. So, the LVDTs with a low-pass filter complements with the inertial sensor with high-pass filter. The pair of low-pass and high-pass filter here are called complementary filters and satisfies the relation $L + H = 1$, where L is the low-pass filter and H is the high-pass filter. Again, similar to the control filter, the complementary filter can take almost any arbitrary shape. Since the discussion here is not on the design of complementary filters, we choose the 4th-order filter designed by Sekiguchi [6] as the starting point. The low-pass filter is

$$L = \frac{35\omega_{\mathrm{b}}^4 s^3 + 21\omega_{\mathrm{b}}^5 s^2 + 7\omega_{\mathrm{b}}^6 s + \omega_{\mathrm{b}}^7}{(s + \omega_{\mathrm{b}})^7}, \tag{5}$$

where $\omega_{\mathrm{b}} = 2\pi f_{\mathrm{b}}$ is the blending angular frequency and $H = 1 - L$ is

$$H = \frac{s^7 + 7\omega_{\mathrm{b}} s^6 + 21\omega_{\mathrm{b}}^2 s^5 + 35\omega_{\mathrm{b}}^3 s^4}{(s + \omega_{\mathrm{b}})^7}. \tag{6}$$

If necessary, a notch filter can be applied to the low-pass which makes the signal to be dominated by the inertial sensor at the particular frequency, as is standard in LIGO [3]. This is particularly useful if the sensor correction is not perfect. With the notch filter, the microseism contribution from the sensor noise can be reduced, improving active seismic isolation performance. If needed, the notch filter is defined as

$$F_{\mathrm{notch}} = \frac{s^2 + (\omega_{\mathrm{notch}} s)/Q + \omega_{\mathrm{notch}}^2}{s^2 + (d\omega_{\mathrm{notch}} s)/Q + \omega_{\mathrm{notch}}^2},$$

where ω_{notch} is the angular frequency where the notch is centered at, Q is the quality factor and d is the depth of the notch.

Alternatively, instead of manually adding a notch filter to the low-pass, we can also defined and augmented high-pass filter

$$H = \frac{s^7 + 7c_1 s^6 + 21c_2^2 s^5 + 35c_3^3 s^4}{(s + c_4)^7}, \tag{7}$$

where c_i are positive coefficients. The pre-factors and exponents are kept so all c_i have the same order of magnitude, which is convenient during optimization. In this wav, the high-pass filter will be guaranteed to be a 4th-order filter. Also, the optimization will automatically generate a notch-like feature in the complementary low-pass filter if applicable. Whereas, if we optimize the low-pass and notch filter instead, the high-pass filter will not be a fourth-order filter which makes it incapable of filtering the $f^{-3.5}$ noise of the geophone.

Fig. 5 shows the sensor noise configuration with inertial sensor involved. It follows that the total sensor noise now becomes

$$N_s = L\left(N_{\mathrm{LVDT}} + H_{\mathrm{sc}}N_{\mathrm{seis}} + \alpha X_{\mathrm{g}}\right) + HN_{\mathrm{inert}}, \tag{8}$$
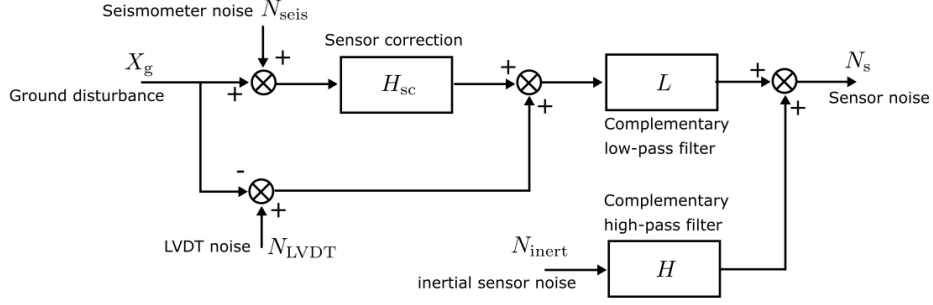
Figure 5: Sensor noise contribution from seismic noise, seismometer noise, LVDT noise and inertial sensor noise with complementary filter topology.

where N_{inert} is the inertial sensor noise. Here, we introduce a constant coefficient α to model imperfect sensor correction. It follows that when $\alpha = 0$, ground noise from LVDT is completely canceled by sensor correction, when $0 < \alpha < 1$, the sensor correction is imperfect, and when $\alpha = 1$, sensor correction is a complete failure. If we want to model the case with no sensor correction, then $\alpha = 1$ and $H_{\text{sc}} = 0$.

The blending frequency of complementary filter is often manually selected based on subjective decisions. For a fair discussion, we propose an objective way to determine the complementary filter. Since the blending filter Eqn.7 is a function coefficients c_i, where $i = 1, 2, 3, ...$, we can introduce a cost function defined by the integrated RMS of the total sensor noise

$$J(c_i) = \sqrt{\int_0^\infty \langle N_s^2 \rangle \, df}. \tag{9}$$

Then, given the noise profiles of LVDT, inertial sensor etc, we can find the optimal complementary filter by minimizing the cost function over the arguments of the cost function

$$H_{\text{opt}} = H\left(\underset{c_i \in \mathbb{R}^+}{\arg\min} \, J(c_i)\right). \tag{10}$$

In this case H_{opt} and $L_{\text{opt}} = 1 - H_{\text{opt}}$ together will give the minimum sensor noise. Here, we emphasize that the frequency range must include low frequency regions where inertial sensing noise dominates. Otherwise, the optimization will give a complementary filter which has unacceptably low blending frequency, which is impractical.

3.2.1 Note

In the beginning of my attempt, the optimization of the complementary filter was over the blending frequency ω_{b} and the notch filter frequency ω_{notch}, quality factor Q and d. But, at the end, I found that the optimization is sometimes not stable and that I was unsuccessful to obtain useful inertial sensor noise requirement using this method. More importantly, the high-pass filter is not guaranteed to have 4th-order attenuation, which basically ruined the purpose of it. Therefore, after countless failed attempts, I switched to optimizing the high-pass filter instead and hope that optimizing the filter over more than one coefficients will automatically generate a notch like filter in the low-pass, which it did in the end. This will guarantee the high-pass filter to have 4th-order attenuation as well as minimizing the seismic contribution in the LVDT signal.

3.3 Control Gain Optimization

In the similar fashion, for known sensor noises and plants, following Eqn. 3, we can set a cost function

$$I(K_{\text{IP}}) = \sqrt{\int_0^\infty \langle X_{\text{IP}}^2 \rangle \, df}, \tag{11}$$

such that the control filter

$$K_{\text{IP,opt}} = \underset{k \in [0, k_{\text{margin}})}{\arg \min} \quad I(K_{\text{IP}}) \tag{12}$$

is an optimal filter $K_{\text{IP,opt}}$ that gives the minimal residual motion at the IP stage. Here, k is a bit ambiguous. In the ideal case, k should be a vector of coefficients that fully determines the filter. However, in this case, we set it as the static gain of the current filter and retain the overall shape of the current filter for simplicity, i.e.

$$K_{\text{IP,opt}} = k_{\text{opt}} K_{\text{IP}},$$

where k_{opt} is some constant that gives the minimum residual motion and K_{IP} is the current damping filter implemented. Nevertheless, we should also take care of the stability of the system. So, the upper bound of k is the gain margin of the current system.

3.4 Control Gain Limitation

The use of inertial sensor itself does not reduce the residual motion contribution from the low frequency seismic noise. But rather, it enables the possibility to increase the control gain achieve active isolation. However, the control gain cannot be increased arbitrarily due to the control noise requirement which, according to Sekiguchi, is $1 * 10^{-19} \, \text{m}/\sqrt{\text{Hz}}$ at $10 \, \text{Hz}$. A quick estimation of the control noise by the current inverted pendulum control yields

$$\sqrt{\langle X_{\text{TM}}^2 \rangle}\Big|_{10\,\text{Hz}} = \left| \frac{X_{\text{TM}}}{X_{\text{IP}}} \right| \sqrt{\langle X_{\text{IP}}^2 \rangle}\Big|_{10\,\text{Hz}} = 2.84 * 10^{-23} \, \text{m}/\sqrt{\text{Hz}},$$

which is rather trivial compared to the requirement. But, let's make it a reference so modifications for further simulations should not deviate much from this value.

Another limitation of the control gain is stability. However, without serious analysis of the system, it is impossible to estimate the true boundary because the control filter can almost take any arbitrary shape. Therefore, for following analyses, we keep the shape of the control filter and only adjust a multiplicative constant. Under this constraint, the gain margin is only roughly 4 (details omitted here). If necessary, the limitation can be eased if we optimize the low-pass filter for the control cut-off. The current filter is a 4th-order Butterworth lowpass with cutoff frequency at $10 \, \text{Hz}$. Without the low-pass filter, the gain margin becomes 21.

3.5 Short Summary of the Strategy

According to the current system, the residual motion requirement of the inverted pendulum is determined by the nominal condition with 50th percentile seismic noise. The integrated RMS requirement is $0.1925 \, \mu\text{m}$ and the band limited (0.1 Hz,1 Hz) integrated RMS requirement is $0.0128 \, \mu\text{m}$. It is a belief that under this condition, lock-acquisition is possible and stable. And, with this reference requirement, in later sections, we shall discuss the inertial sensor noise requirement when the seismic noise is higher or when sensor correction isn't perfect. We leave the possibility of redesigning the control filter shape and complementary filter for further improvement of control performance. Rather, we limit ourselves do adjustment according to the optimization approaches as to minimize sensor noise and residual motion. In principle, we can wrap another optimization around those two to obtain the inertial sensor noise requirement. However, we are worried that the nested optimization will take a very long time to converge. Instead, we do complementary filter and control gain optimization across a list of inertial sensor noise, and see what level of sensor noise will give residual motion that meets the requirement.

4 Result

4.1 Inertial Sensor Noise Requirement without Sensor Correction

Without sensor correction, the LVDT readout is coupled to the ground noise. Hence, with the complementary filter configuration the seismic noise coupling is $\alpha = 1$ and the sensor correction filter is $H_{\rm sc} = 0$. The total sensor noise reads

$$N_{\rm s} = L\left(N_{\rm LVDT} + X_g\right) + H N_{\rm inert},$$

where H is the $4^{\rm th}$-order complementary high-pass filter given by Eqn. 7 and L is the corresponding complementary low-pass filter.

4.1.1 Under $50^{\rm th}$ Percentile Seismic Noise

If we use the typical values for LVDT and geophone noise in table. 1, and assume $50^{\rm th}$ seismic noise, we see that the sensor noise is much higher than of the current sensor correction configuration. So, it follows that if we optimize the control gain to minimize the residual motion, the residual motion level should be higher. In this case, optimization gives an integrated RMS of $0.0799\,\mu$m and band limited (0.1 Hz, 1 Hz) RMS of $0.0258\,\mu$m. Since the band limited RMS is higher than the requirement, we further simulated the results for cases with lower geophone noise and hope to find a geophone noise level low enough to give a residual motion that meets the requirement. Here, we choose N_0 in the set $\{2*10^{-6}, 1*10^{-6}, 5*10^{-7}, 2.5*10^{-7}, 1.25*10^{-7}, 6.25*10^{-8}\}$. In these cases, we optimized the control gain over both integrated RMS and band limited RMS. The residual motion result of different levels of geophone noise is shown in Fig. 6 As can be seen, in both cases, the integrated RMSs are well below the requirement.
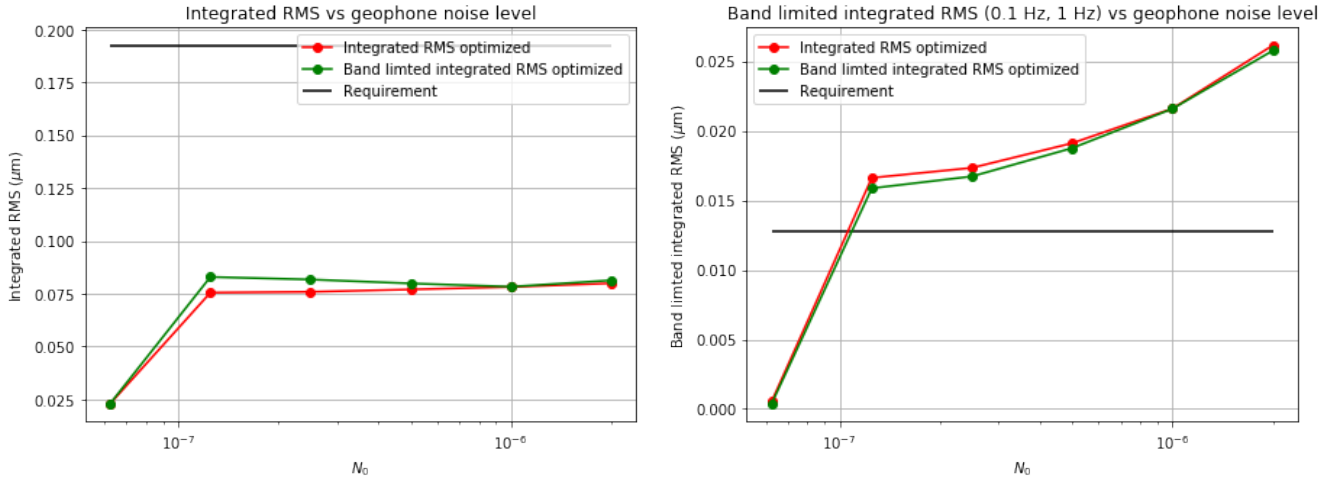
Figure 6: Left: Best integrated RMS results with 6 different inertial sensor noise under $50^{\rm th}$ seismic noise. Right: Best band limited integrated RMS (0.1 Hz, 1 Hz).

However, the band limited RMS in all cases of geophone noise can't meet the requirement unless the noise becomes unrealistically low and with blending frequency impractically low. The same is true even if the optimization is over the band limited RMS. Moreover, as the geophone noise level decreases, the best band limited RMS saturates at a value around $0.0159\,\mu$m. It is not until the geophone noise level becomes ridiculously low that the residual motion requirement can be met. So, it appears that the requirement is unlikely to be met with realistic geophone noise under a simple complementary filter.

As a reference, the noises, optimized filters and open loop gains are shown in Fig. 7. It is worth noting that, from the top right subplot, the optimization over the high-pass filter gives a notch-like feature in the low-pass around microseism frequency as expected.
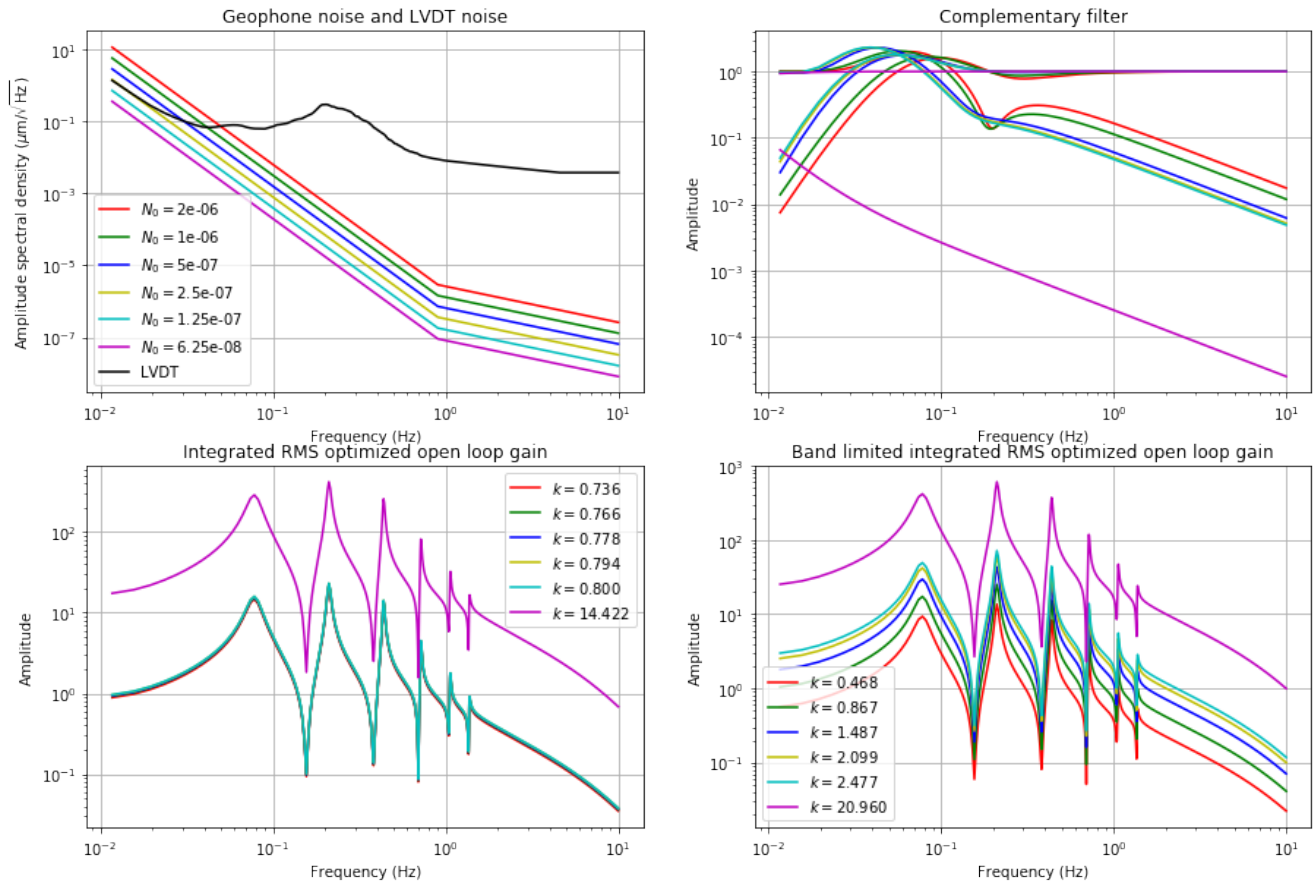
Figure 7: Under 50th percentile seismic noise without sensor correction. Top left: LVDT noise and the candidate geophone noises. Top right: Best complementary filters each correspond to a candidate geophone noise. Bottom left: Open loop gains optimized over the intergrated RMS. Bottom right: Open loop gains optimized over the band limited RMS.

4.1.2 Under 90th Percentile Seismic Noise

Base on the results from last section, we know that this configuration wouldn't be able to withstand 50th percentile seismic noise, and definitely we cannot withstand seismic noise of 90th percentile. But, we put our results here for reference anyway.
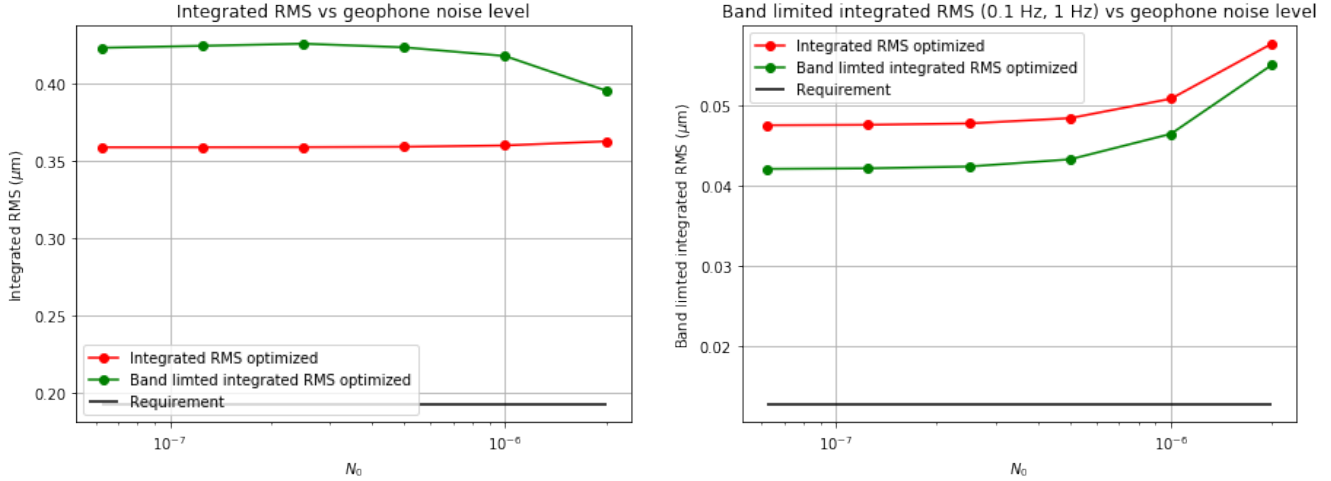
Figure 8: Left: Best integrated RMS results with 6 different inertial sensor noise under 90th seismic noise. Right: Best band limited integrated RMS (0.1 Hz, 1 Hz).
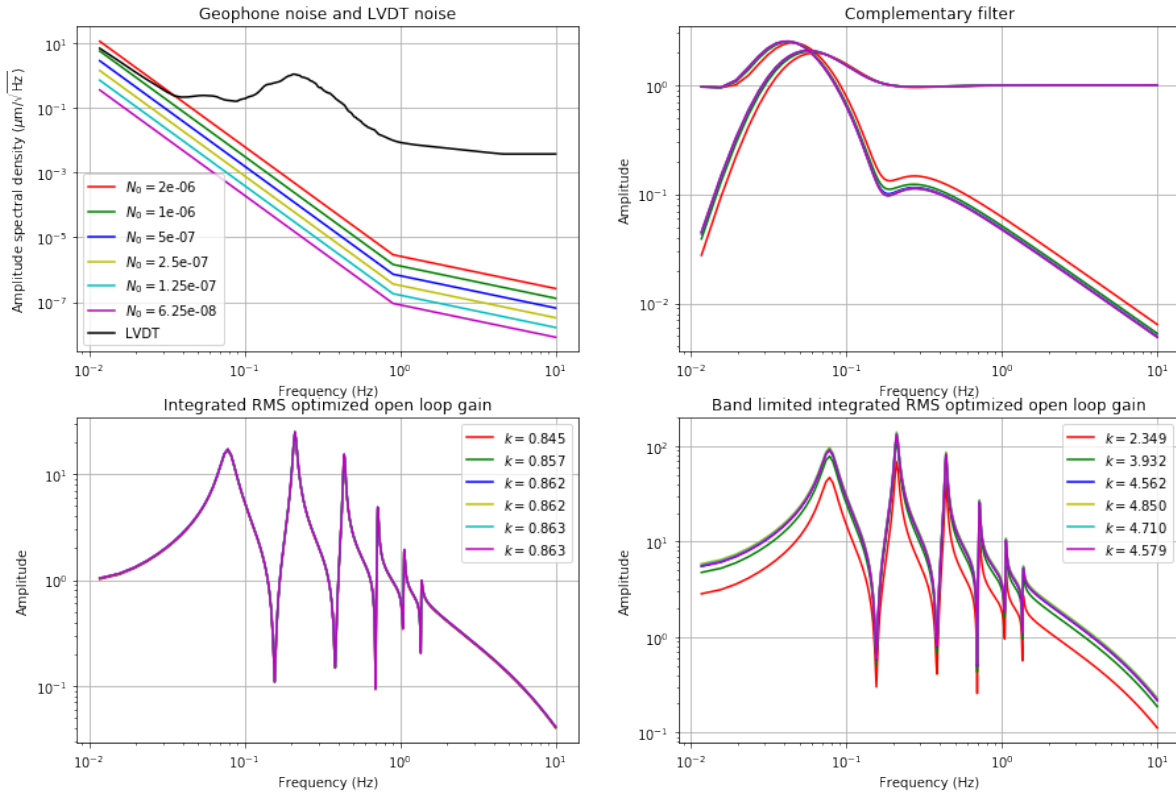
Figure 9: Under 90th percentile seismic noise without sensor correction. Top left: LVDT noise and the candidate geophone noises. Top right: Best complementary filters each correspond to a candidate geophone noise. Bottom left: Open loop gains optimized over the intergrated RMS. Bottom right: Open loop gains optimized over the band limited RMS.

4.2 Inertial Sensor Requirement with Flawed Sensor Correction

With sensor correction, the seismic noise coupling from the LVDT signal can be reduced. However, the cancellation is often not perfect for due to calibration error. In such configuration, the total sensor noise is given by Eqn. 8 which reads

$$N_s = L\left(N_{\text{LVDT}} + H_{\text{sc}}N_{\text{seis}} + \alpha X_{\text{g}}\right) + HN_{\text{inert}}.$$

We explore the inertial sensor noise requirement in two cases of α, namely $\alpha = 0.4$ and $\alpha = 0.1$. The rationale for choosing these two values is obvious according to experiences of current sensor correction. In experience, we have been successful in reducing the residual motion at microseism by 2.5 to 10 times according to [7, 8]. Hence, we assume that we can reduce seismic noise coupling from the LVDT readout at worst to 40% ($\alpha = 0.4$) and at best to 10% ($\alpha = 0.1$). One reason for such residual coupling is due to inter-calibration error between the LVDT and the seismometer. We shall refer this to inter-calibration mismatch from now on. In addition, we will also explore what value of inter-calibration mismatch α can we tolerate with the current sensor noise level.

4.2.1 Under 50th Percentile Seismic noise with 40% Sensor Correction Inter-calibration Mismatch

With a coarse scan of geophone noise levels, we found that the residual motion requirements can be met with geophone noise level between $N_0 = 2 * 10^{-6}$ and $N_0 = 1 * 10^{-6}$. We further did a fine scan with 10 more values linearly spaced between those two values to obtain a more accurate requirement. Results are shown as follows.
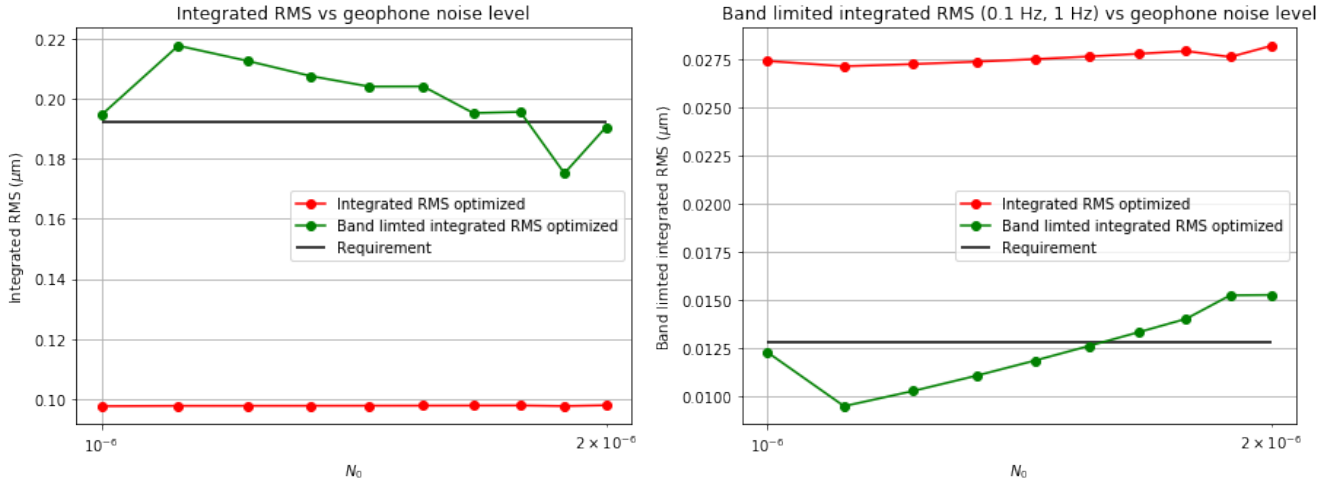
Figure 10: Left: Best integrated RMS results with 10 different inertial sensor noise under 50th seismic noise assuming 40% inter-calibration mismatch. Right: Best band limited integrated RMS (0.1 Hz, 1 Hz).

As can been seen from Fig. 10, the residual motion requirements can be met with geophone noise level at between $N_0 = 1.556 * 10^{-6}$ and $N_0 = 1.667 * 10^{-6}$. Further analysis gives a requirement of $N_0 \approx 1.58 * 10^{-6}$ which is 21% lower than that of the current geophone sensor noise level $2 * 10^{-6}$. The corresponding complementary filters and control gains are shown in Fig. 11. In this case, we need to increase the control gain by 3.432 times.
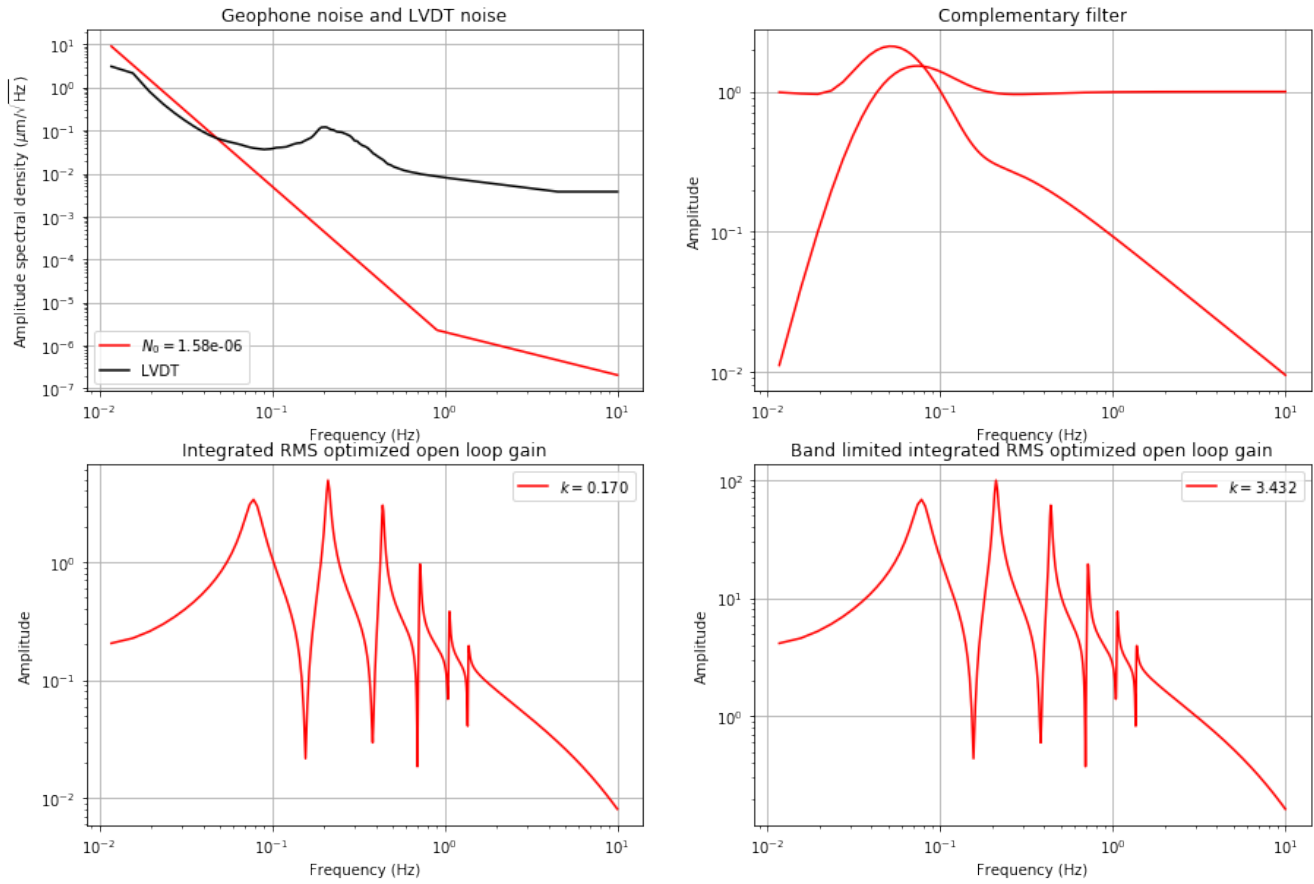
Figure 11: Under 50th percentile seismic noise with sensor correction of 40% inter-calibration mismatch. Top left: LVDT noise and the candidate geophone noises. Top right: Best complementary filters each correspond to a candidate geophone noise. Bottom left: Open loop gains optimized over the intergrated RMS. Bottom right: Open loop gains optimized over the band limited RMS.

4.2.2 Under 90th Percentile Seismic noise with 40% Sensor Correction Inter-calibration Mismatch

Under 90th percentile seismic noise, we once again found that it is impossible to satisfy the residual motion requirement under the condition of 40% inter-calibration mismatch. At the beginning, the optimization is limited by the gain margin. However, even if we ease the gain margin limitation and assume that we can reshape the filter, the requirements are still difficult to be satified. The results are shown below. From Fig. 12, we found that the band limited intergrated RMS saturates at around $0.018\,\mu$m with decreasing geophone sensor noise. This means that the requirements cannot be met unless the geophone noise level is arbitrary low.
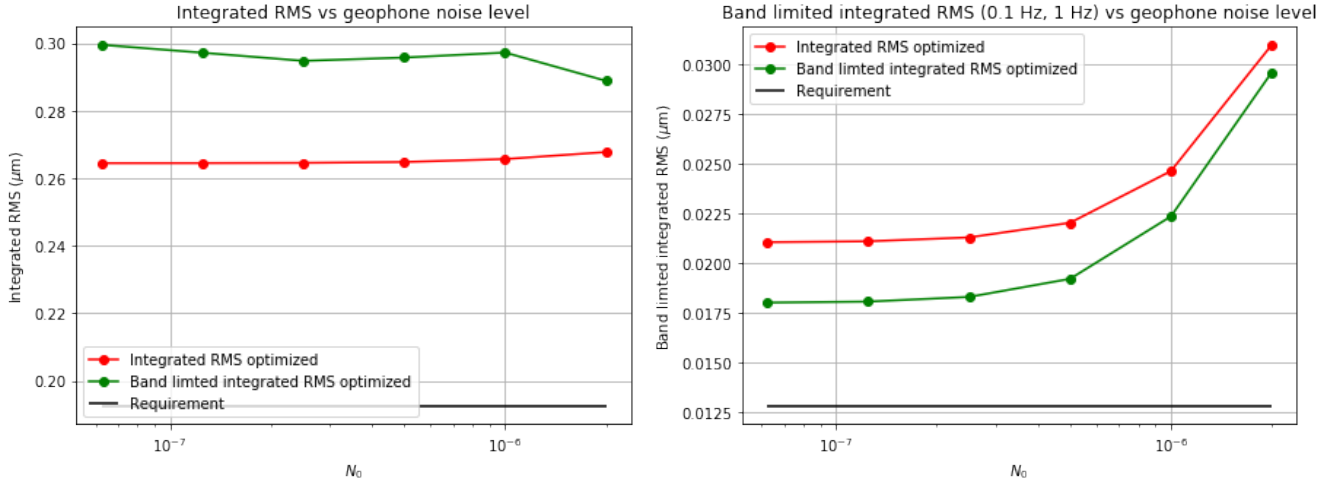
Figure 12: Left: Best integrated RMS results with 6 different inertial sensor noise under 90th seismic noise assuming 40% inter-calibration mismatch. Right: Best band limited integrated RMS (0.1 Hz, 1 Hz).
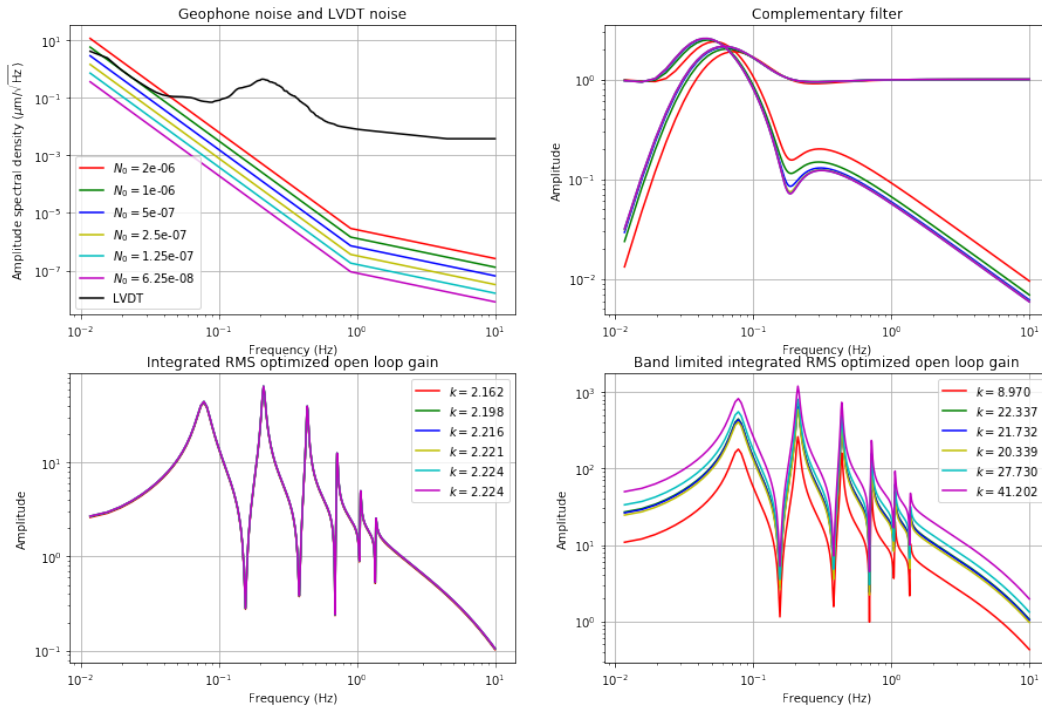
Figure 13: Under 90th percentile seismic noise with sensor correction of 40% inter-calibration mismatch. Top left: LVDT noise and the candidate geophone noises. Top right: Best complementary filters each correspond to a candidate geophone noise. Bottom left: Open loop gains optimized over the intergrated RMS. Bottom right: Open loop gains optimized over the band limited RMS.

4.2.3 Under 50th Percentile Seismic noise with 10% Sensor Correction Inter-calibration Mismatch

Under 90th percentile seismic noise, a rough scan of geophone noise shows that the residual motion requirements can be met with geophone between $N_0 = 4*10^{-6}$ and $N_0 = 8*10^{-6}$. The residual motion results of finer scan is shown in Fig. 14. As can be seen, the residual motion requirement is satisfied with geophone noise level of around $7.55*10^{-6}$. The corresponding filters are shown in Fig. 15. In this case, the blending frequency goes as high as $700\,\text{mHz}$ and the band limited RMS optimized gain is 2.944.
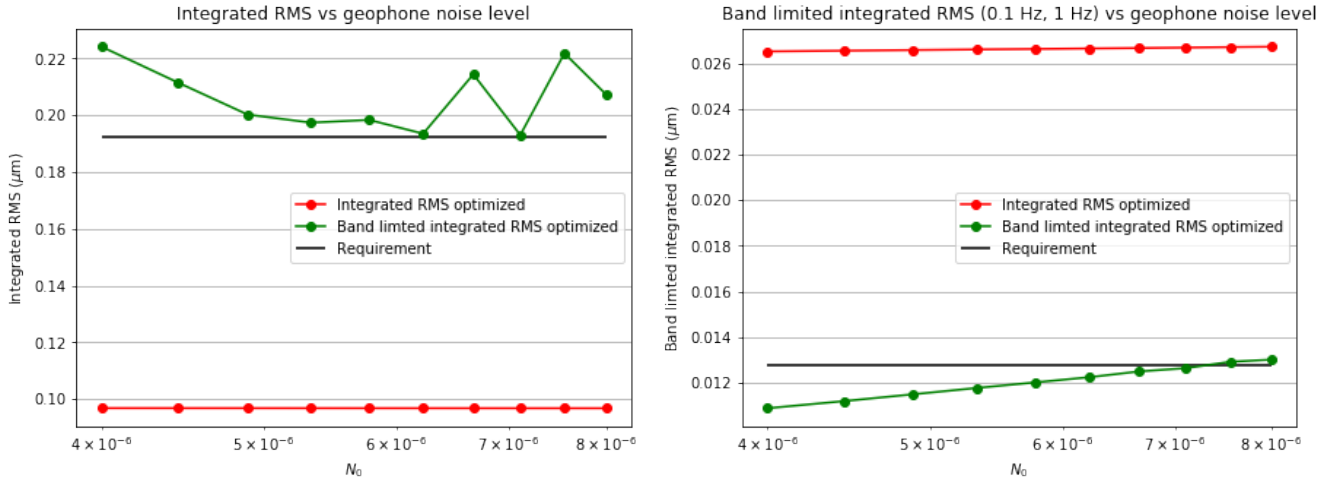
Figure 14: Left: Best integrated RMS results with 10 different inertial sensor noise under 50th seismic noise assuming 10% inter-calibration mismatch. Right: Best band limited integrated RMS (0.1 Hz, 1 Hz).
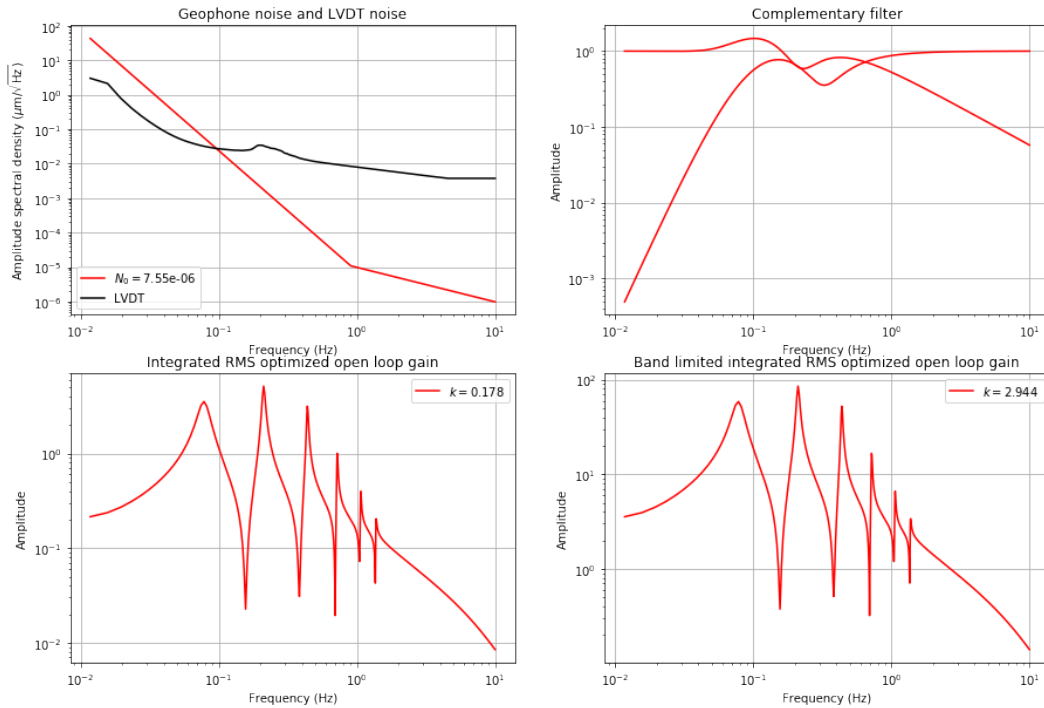
Figure 15: Under 50th percentile seismic noise with sensor correction of 10% inter-calibration mismatch. Top left: LVDT noise and the candidate geophone noises. Top right: Best complementary filters each correspond to a candidate geophone noise. Bottom left: Open loop gains optimized over the intergrated RMS. Bottom right: Open loop gains optimized over the band limited RMS.

4.2.4 Under 90th Percentile Seismic noise with 10% Sensor Correction Inter-calibration Mismatch

For 90th percentile seismic noise, we found that the geophone noise level requirement is between $N_0 = 1 * 10^{-6}$ and $N_0 = 2 * 10^{-6}$, as shown in Fig. 16. Again, we did a fine search and found that the requirement is $N_0 = 1.7 * 10^{-6}$, which is 15% lower than the current value. The filters are shown in Fig. 17. Note that the required gain is 30.2 times higher than the current gain. In addition, the required gain is higher than the current gain margin, meaning that we must redesign the filter in order to maintain the stability of the system.
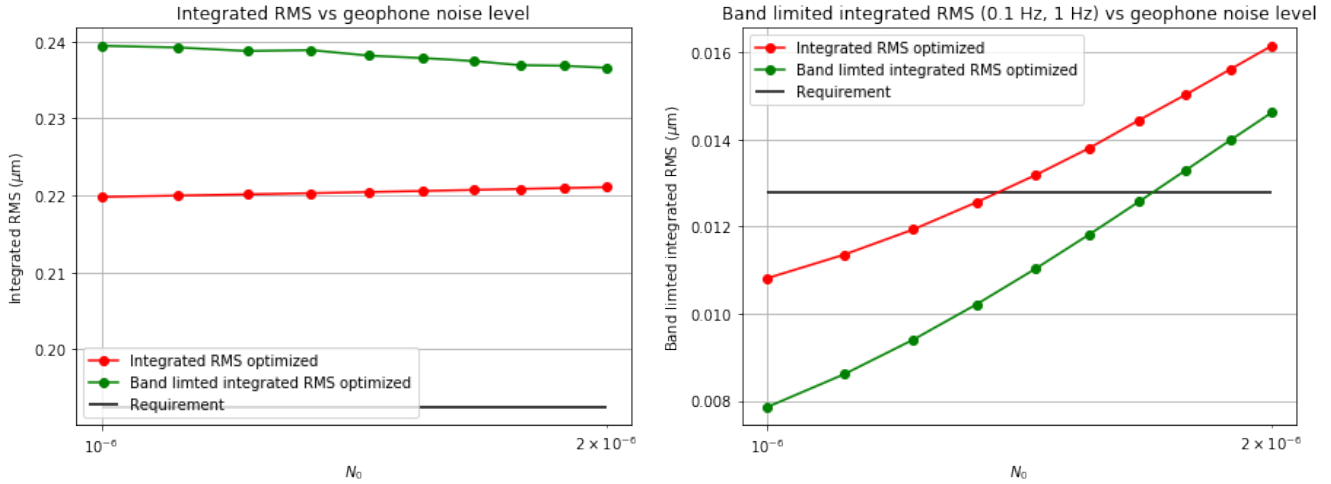
Figure 16: Left: Best integrated RMS results with 10 different inertial sensor noise under 90th seismic noise assuming 10% inter-calibration mismatch. Right: Best band limited integrated RMS (0.1 Hz, 1 Hz).
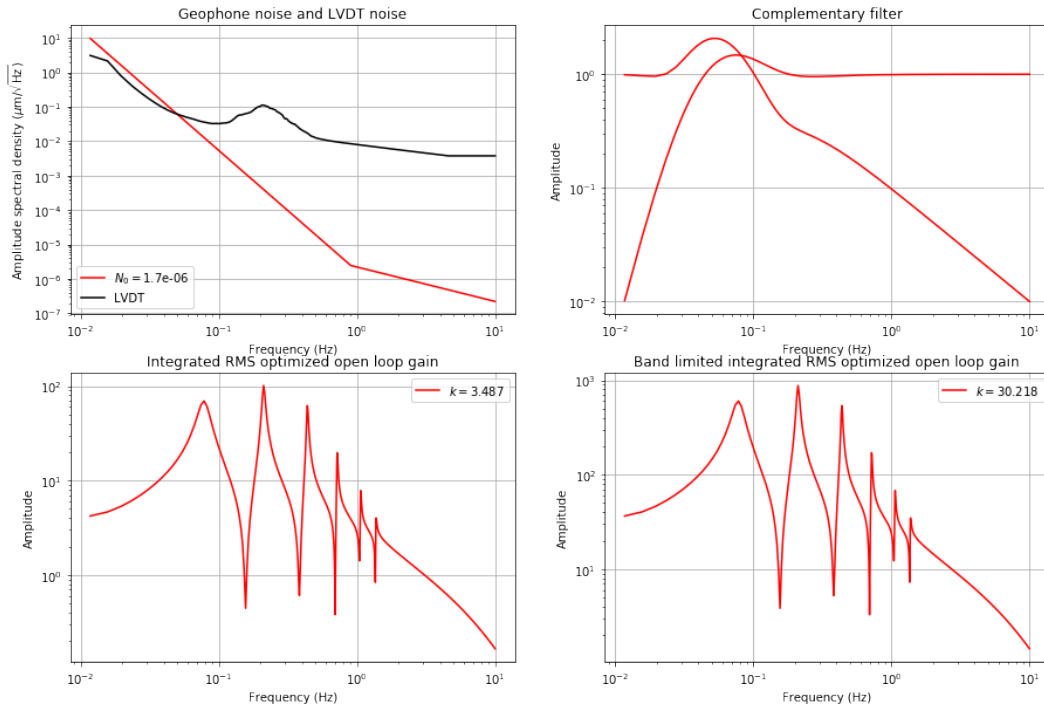
Figure 17: Under 90th percentile seismic noise with sensor correction of 10% inter-calibration mismatch. Top left: LVDT noise and the candidate geophone noises. Top right: Best complementary filters each correspond to a candidate geophone noise. Bottom left: Open loop gains optimized over the intergrated RMS. Bottom right: Open loop gains optimized over the band limited RMS.

4.2.5   Inter-calibration Mismatch Tolerance with Typical Geophone Noise Level

If upgrading inertial sensors is not an option, then the proper question to ponder is perhaps not "What is the inertial sensor requirement?", but "What is the Inter-calibration mismatch requirement". In one of Fujii's klogs [2], he mentioned that the target inter-calibration mismatch would be 10%. From last section, we showed that under 10% of seismic noise coupling, the typical geophone noise level ($N_0 = 2 * 10^{-6}$) is still slightly higher than the requirement $N_0 = 1.7 * 10^{-6}$. So, the only way to get around upgrading inertial sensors is to improve the inter-calibration. We optimize the filters under the condition of 90th percentile seismic noise and with the typical geophone noise level. Instead of incrementally changing the geophone noise level, we ran the optimization with 10 mismatch values ranging from 0.01 to 0.1.
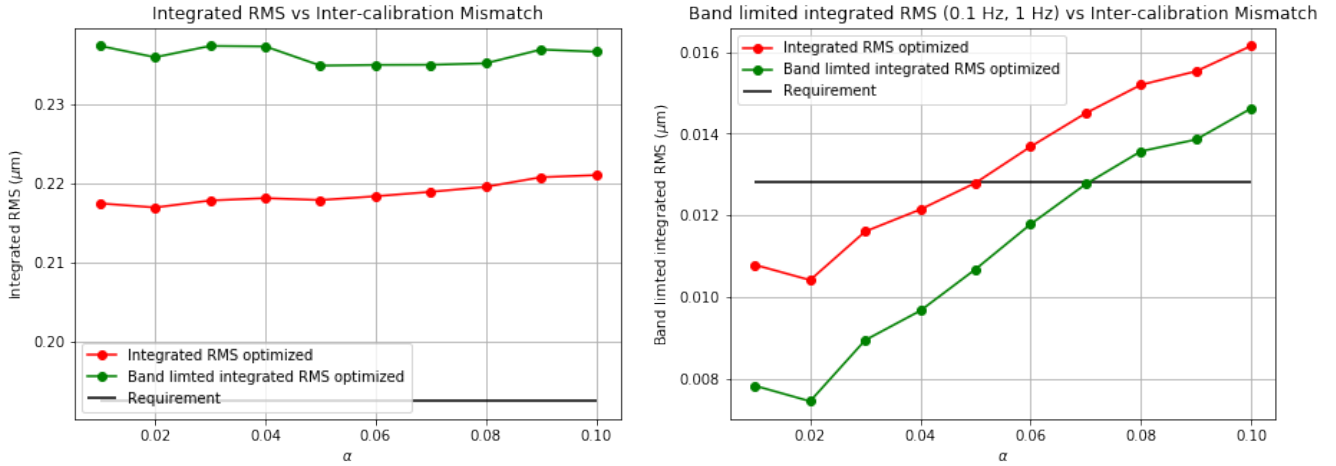
Figure 18: Left: Best integrated RMS results with 10 different sensor correction inter-calibration mismatch under 90th seismic noise and typical geophone noise. Right: Best band limited integrated RMS (0.1 Hz, 1 Hz).

As shown in Fig. 18, it turned out that, with the typical geohpone noise and optimized filters, we can tolerate roughly 7% of inter-calibration mismatch, which is not too bad from the target which Fujii set. As the same as before, under 90th percentile seismic motion, the required gain is around 30 higher than the current one and exceeds the gain margin. So, if we need to sustain such high ground disturbance, redesigning the control filter is a must.
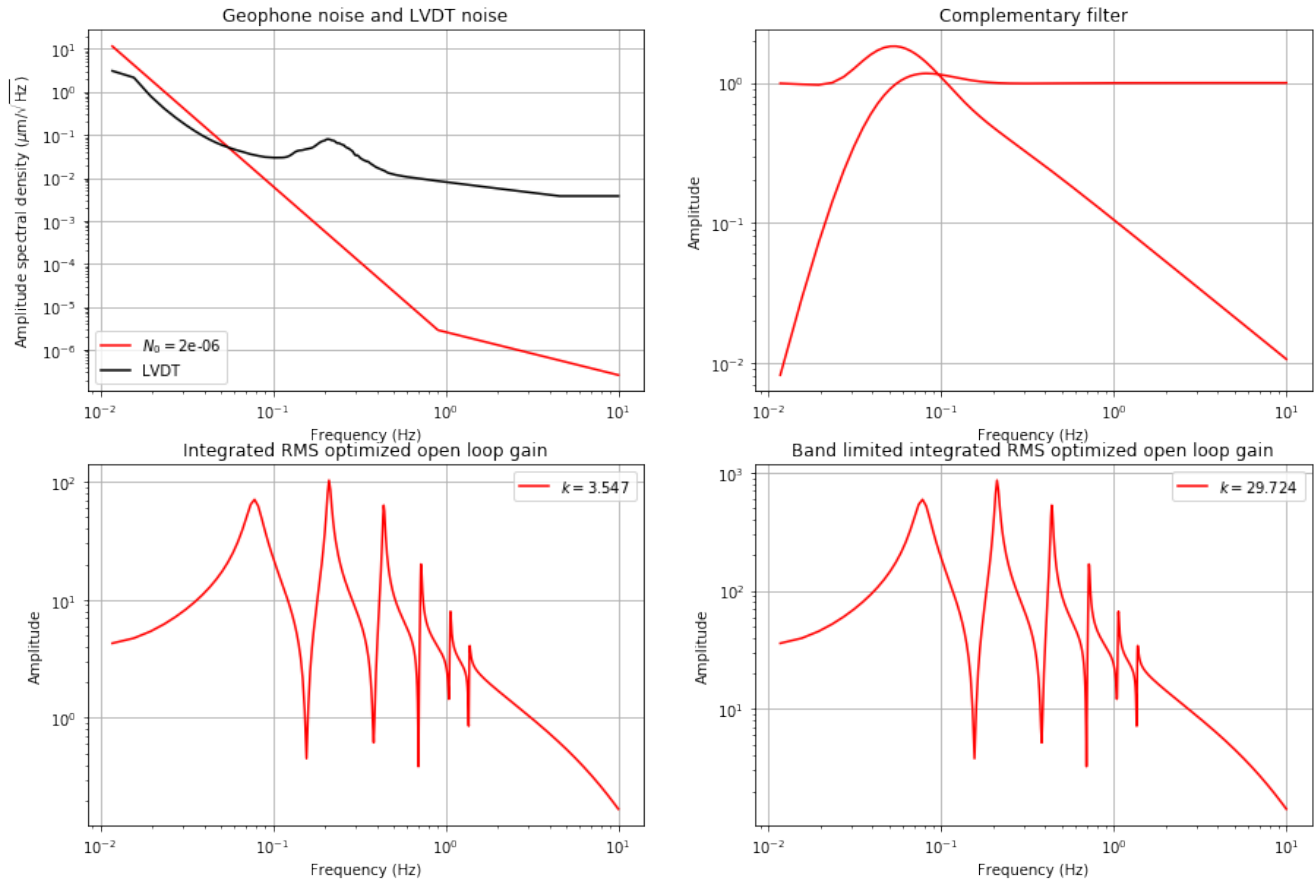
Figure 19: Under 90th percentile seismic noise with sensor correction of 7% inter-calibration mismatch. Top left: LVDT noise and the candidate geophone noises. Top right: Best complementary filters each correspond to a candidate geophone noise. Bottom left: Open loop gains optimized over the intergrated RMS. Bottom right: Open loop gains optimized over the band limited RMS.

4.3   Summary

Using the optimization method, we derived the inertial sensor noise requirements with and without sensor correction under both 50th and 90th percentile seismic noise. Table. 2 gives a summary of geophone noise requirement under the condition of no sensor correction and with sensor correction with 40%, 10% and 7% inter-calibration mismatch. We found that the typical geophone noise can tolerate 7% of sensor correction calibration mismatch.

Seismic noise percentile	50th	90th
No sensor correction	N/A[1]	N/A[1]
Sensor correction with 40% inter-calibration mismatch	$1.58 * 10^{-6}$	N/A[1]
Sensor correction with 10% inter-calibration mismatch	$7.55 * 10^{-6}$	$1.7 * 10^{-6}$
Sensor correction with 7% inter-calibration mismatch	N/A [2]	$2 * 10^{-6}$

Table 2: Geophone noise requirement with under different configuration.

We also discovered that the optimal gain under 50th percentile seismic noise is around 3 times higher than that of the damping filter installed in ITMY. Furthermore, the required gain under 90th percentile seismic noise is approximately 30 times the one in ITMY. Since the gain margin of the particular filter is around 21, the current filter must be modified in order to increase the gain margin in the case of 90th percentile seismic noise.

5   Discussion

In the very beginning of the document, we set the residual motion requirement to be that of current configuration, which is simply LVDT with sensor correction under 50th percentile seismic noise. While this is not the true requirement, it serves as a golden standard for discussing configurations that are comparable, if not better. In all cases, we found that with better sensor correction the requirement for inertial sensing noise is lessen. In particular, we found that the noise requirement would be unrealistically high without sensor correction, whereas with sensor correction with 7% of inter-calibration mismatch, we would be able to use the current hardware to suppress the inverted pendulum motion under 90th percentile seismic noise to an extent equivalent to that of the current system under 50th percentile seismic noise. Therefore, besides improving inertial sensors, improving sensor correction also plays an important role in preserving interferometer lock against high level of seismic noise and should be dealt with perfection.

The suggested inertial sensor noise requirements are conservative. Again, we emphasize that the inverted pendulum residual motion requirement that we estimated here is by no means the true requirement. It is only a pessimistic estimation based on the hypothesis that the current ITMY configuration has enough suppression to the suspension motion such that interferometer lock is stable under 50th percentile seismic noise. It is expected that the actual residual motion requirement is not as strict. Therefore, the inertial sensor noise requirements from the simulated results might also be not as strict. Moreover, throughout the discussion, we limited the complementary filter and control filter to take certain limited forms. If these restrictions are relieved, then better performance can certainly be achieved. Also, if we consider other type of inertial sensors, the results can be completely different. Nevertheless, we showed that under such restrictions, we will be able to meet the interforemeter lock-acquisition condition with current hardware if sensor correction mismatch is under 7%.

We showed that we will need to increase the control gain by 3000% in the case of 90th percentile seismic noise. This means that modification of the damping filter is inevitable since 3000% exceeds the gain margin of the current filter. More importantly, the we see an emerging need of adaptive control because the optimal gain at 50th percentile seismic noise only 300% higher than the current filter. So, we need an adaptive mechanism that can automatically adjust the control filter as the seismic noise evolves and this shall be one of my focus in the coming visit.

---

[1]Could not meet requirement.
[2]Trivial case, did not investigate.

References

[1] Trillium compact 120-sv1 information.
Available at `https://gwdoc.icrr.u-tokyo.ac.jp/cgi-bin/private/DocDB/ShowDocument?docid=8440`.

[2] Y. Fujii. Itmy response in l?
Available at `http://klog.icrr.u-tokyo.ac.jp/osl/?r=13333`.

[3] Fabrice Matichard, B. Lantz, Richard Mittleman, Kenneth Mason, J. Kissel, J. McIver, B. Abbott, R. Abbott, S. Abbott, E. Allwine, Sam Barnum, Jessica Birch, Sebastien Biscans, Charles Celerier, D. Clark, Dennis Coyne, Dan Debra, R. DeRosa, Matthew Evans, and Shiping Wen. Seismic isolation of advanced ligo: Review of strategy, instrumentation and performance. *Classical and Quantum Gravity*, 32, 02 2015.

[4] K. Miyo. Seismic noise of kagra mine.
Available at `https://gwdoc.icrr.u-tokyo.ac.jp/cgi-bin/private/DocDB/ShowDocument?docid=10436`.

[5] Nanometrics. Trillium compact.
Available at `https://www.nanometrics.ca/products/seismometers/trillium-compact`.

[6] T. Sekiguchi. *Study of Low Frequency Vibration Isolation System for Large Scale Gravitational Wave Detectors*. PhD thesis, Tokyo U., 2016.

[7] A. Shoda. Correct sc factor reduced the rms of fb signal :).
Available at `http://klog.icrr.u-tokyo.ac.jp/osl/?r=13439`.

[8] L. Trozzo. Comment to correct sc factor reduced the rms of fb signal :).
Available at `http://klog.icrr.u-tokyo.ac.jp/osl/?r=13441`.

[9] L. Trozzo. Ex ip: Lvdt and geo noise estimation.
Available at `http://klog.icrr.u-tokyo.ac.jp/osl/index.php?r=7422`.

[10] L. Trozzo. Ey ip: Lvdt and geo noise estimation.
Available at `http://klog.icrr.u-tokyo.ac.jp/osl/?r=8568`.

6 Appendix

Here are some obsoleted sections.

6.1 Limitation by Preisolator Actuation Resolution

In the ideal case, the preisolator displacement caused by the feedback actuation perfectly balances the displacement caused by the seismic noise disturbance. In reality, this is not possible because the actuators do not have infinite resolution, meaning that they are not infinitely delicate. This also means that the sensor sensitivity beyond the actuator resolution will not be useful for feedback control since the actuators will not be able to cancel what the sensor measures. So, the smallest displacement we would be able to actuate is the actuation efficiency multiplied by the DAC noise. This gives the lower bound of the sensitivity requirement of our sensor,

$$\sqrt{\langle N_{\mathrm{s}}^2 \rangle} = |P_{\mathrm{IP}}| \sqrt{\langle N_{\mathrm{DAC}}^2 \rangle},$$

where $\sqrt{\langle N_{\mathrm{s}}^2 \rangle}$ is the amplitude spectral density (ASD) of the noise, P_{IP} is the inverted pendulum transfer function and $\sqrt{\langle N_{\mathrm{DAC}}^2 \rangle}$ is the ASD of the DAC noise. So we have some meaningful requirement here, where any sensitivity lower than this is not useful in helping active isolation.

Show some figures here.

6.2 Inertial Sensor Noise Requirement without Sensor Correction ($\alpha = 1$, $H_{\text{sc}} = 0$) under an Augmented 4th-order Complementary Filter

As shown in last section, using a simple complementary filter would requirement impractically low inertial sensing noise in order to meet the residual motion requirement. Therefore, we proposed to combine a notch filter with the complementary low pass. In doing so, we hope that the notch will rapidly reduce the microseism contribution from the total sensor noise, enabling more active isolation with the inertial sensor. We do the same iterations as the previous section and obtained the residual motion results as shown in Fig. 20. From the figure, the integrated RMS
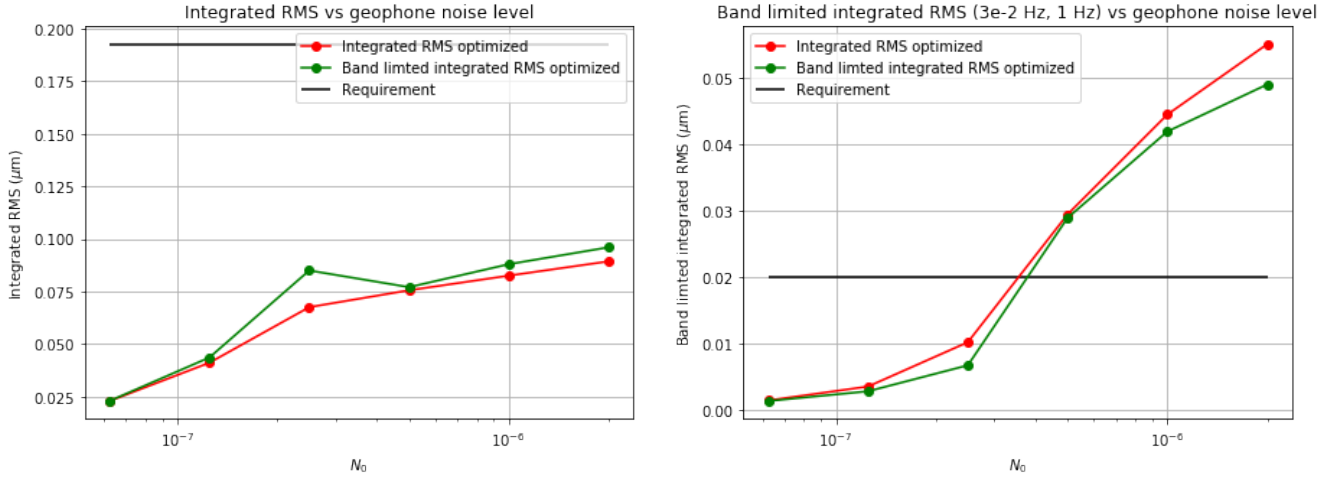
Figure 20: Left: Best integrated RMS results with 6 different inertial sensor noise under 50th seismic noise with a complemetary filter augmented with notch filter. Right, Best band limited integrated RMS under the same condition.

requirement can be met easily again in all cases. What is more, the band limited integrated RMS requirement can also be met with geophone noise level below some N_0 midway between $2.5 * 10^{-7}$ and $5 * 10^{-7}$. To obtain a more precise estimate of the geophone noise requirement, we do the same fine iteration with with 10 values of N_0 linearly spaced between the two bounds. The residual motion results are shown in Fig. 21.
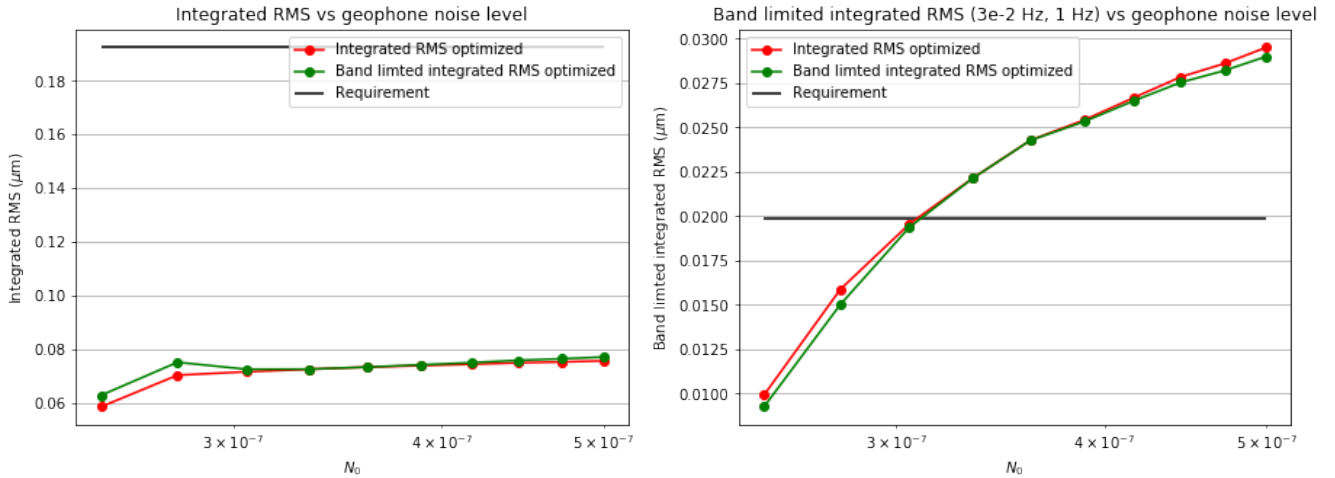
Figure 21: Left: Best integrated RMS results with 10 different inertial sensor noise levels between $N_0 = 2.5 * 10^{-7}$ and $N_0 = 5 * 10^{-7}$ under 50th seismic noise with a complemetary filter augmented with notch filter. Right, Best band limited integrated RMS under the same condition.
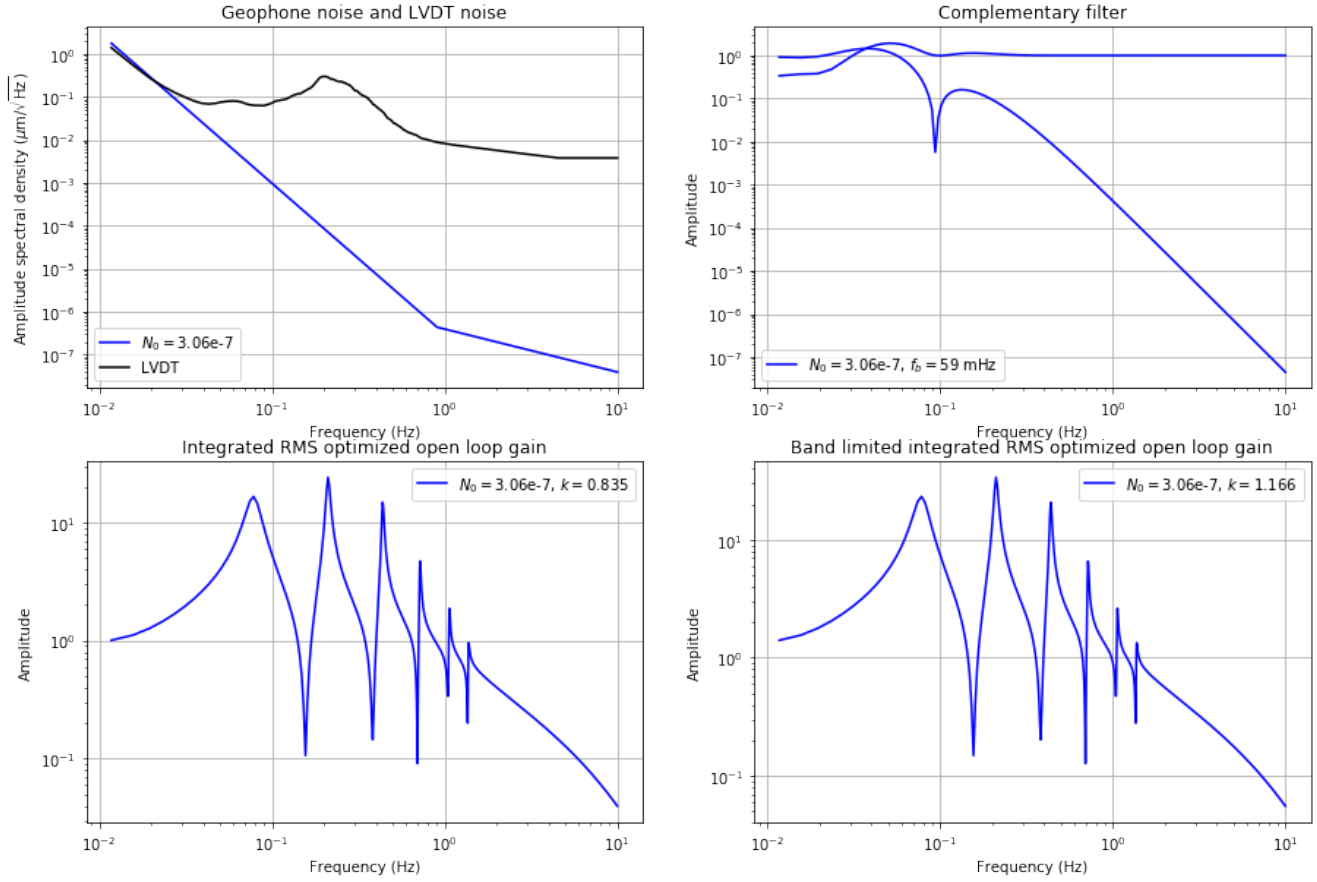
Figure 22: Results of the geophone noise that satisfies the invented pendulum residual motion requirement with corresponding optimized filters.

As it turns out, the band limited residual motion requirement can be met if the geophone noise level N_0 goes down to around $3.06 * 10^{-7}$, which is almost 1 order of magnitude lower than that of the current geophones $(2 * 10^{-6})$.

As a reference, the noises, optimized filters and open loop gains for this case are shown in Fig. 22. As can be seen, if we allow a notch to be applied to the complimentary low-pass filter, then we will be able to meet the residual motion requirement of the inverted pendulum with a geophone noise level at $N_0 = 3.06 * 10^{-7}$. In this case, the optimal blending frequency is at $59\,\mathrm{mHz}$ and the optimal gain is 1.166 times the current control filter.

6.3   Augmented 4th-order Complementary Filter under 90th Percentile Seismic noise without Sensor Correction

So far, we have been discussing the inertial sensing noise requirement under the 50th seismic noise. In the case of simple 4th-order complementary filter, the requirement couldn't be met and hence we know for sure that such configuration will not be able to withstand nominal ground motion, let alone a higher level of seismic noise. So, we proceed to investigate the performance of using the augmented complementary filter under 90th percentile seismic noise.

Using the previous set of N_0s, we estimated the best residual motions from the same optimization procedures. In Fig 23, both integrated RMS and band limited RMS requirements can be met surprisingly with only geophone noise level of $N_0 = 5*10^{-7}$, which is higher than that in the case of 50th percentile seismic noise. However, there are some caveats to be noted, and to some extent, the results are false. As shown in Fig. 24, the geophone noises are almost always lower than that the LVDT. This means that the optimization of the complementary filter will give a result of which sensing signal is dominated by the geophone signal. As can be seen in the same figure, at the top right subplot, the notch filters are heavily distorted such that the actualy blending frequencies go way lower than what is plotted.

In practice, it is almost impossible to blend the signals at such low frequencies. Therefore, the result of the inertial sensing noise requirement is very not believable as those filters are not implementable. Yet, this doesn't mean that we cannot obtain a useful requirement under 90th percentile seismic noise. This is because we are limiting the filter shapes for all cases. The result could have been entirely different if we were allowed to optimize also the shape of the filters. But, again, the design of filters is not in the scope of this report. In conclusion, using our method, we are not able to give an accurate estimate of inertial sensor requirement that guarantees good residual motion of the inverted pendulum.

Nevertheless, evidently, our system is capable of suppressing the microseism at 90th percentile seismic noise. If we focus on the case where $N_0 = 1*10^{-6}$, from the right subplot of Fig .23, the band limited residual motion can be met. And, from the bottom right subplot of Fig. 24, we see that the band limited RMS requirement can be met with only an additional static gain of around 13.9, which is well below the gain margin. This is a very good evidence that we should be able to withstand 90th percentile seismic noise with proper filter design and with good enough sensor or sensor correction.
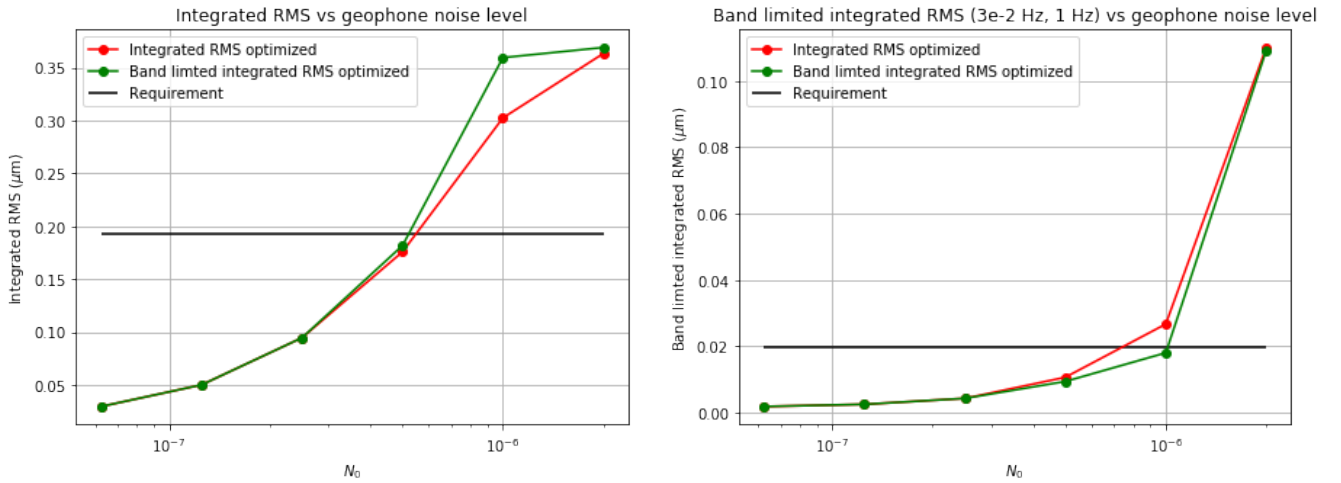
Figure 23: Residual motion with 90th percentile seismic noise under optimized complementary filter and gains. Left: Integrated RMS. Right: Band lmited integrated RMS.

Figure 24